Trans. Indian Inst. Met. manuscript No.
(will be inserted by the editor)

Comparison of continuum damage laws under uniaxial creep for an AISI 316 Stainless Steel

Tejas Ranjekar · **Sivasambu Mahesh**

Received: date / Accepted: date

Abstract Parameters of five popular continuum damage models are fit to match their creep rate and time to rupture predictions with that of a validated micro-mechanisms based model at a high nominal stress for an austenitic stainless steel. Their predictions are then compared with that of the micro-mechanisms based model at lower stress levels. The creep-strain rate and time to failure predictions of the model due to Wen et al. [1] best agrees with that of the micro-mechanisms based model in the regime of dominance of creep deformation processes. At still lower stress levels, where cavitation-rate is determined by diffusion processes, the Wen et al. model predictions of creep lifetimes become excessively non-conservative. A correction based on a formula due to Cocks and Ashby [2] is proposed for this regime.

Keywords Creep · Continuum Damage Mechanics · Damage micro-mechanisms · 316-type Austenitic Stainless steels

T. Ranjekar · S. Mahesh

Department of Aerospace Engineering, Indian Institute of Technology, Madras, Chennai 600036.

1 Introduction

Creep in austenitic stainless steels occurs by the interacting mechanisms of cavitation, and wedge-cracking at grain boundary facets, whose rates are controlled both by diffusion and deformation processes [3, 4]. The dominance of a particular mechanism depends on the load and temperature levels. At homologous temperatures of about 0.4, at high stresses, creep rupture under constant uniaxial tensile load occurs by transgranular necking under an exponentially increasing creep rate [5]. At intermediate loads, elongation at the point of creep failure reduces, and failure switches to a brittle intergranular character [6]. Intergranular cavitation at grain boundaries, linking up to form wedge cracks near triple junctions [7], and possibly accelerated by grain boundary sliding [8] dominates in this regime. Even though the failure in this regime is dominated by the growth of cavities by diffusion of atoms away from cavities, the growth rate is itself constrained by the creep deformation of the surrounding material [9]. Finally, at very low loads, creep strains and grain boundary sliding become negligible. This regime is of importance, because service conditions typically fall within this regime [3, Fig. 6]. Cavity growth occurs in this regime by diffusional mechanisms only.

A detailed micro-mechanisms based model for an AISI 316 stainless steel is available in the literature [10]. In this model, the polycrystalline material is assumed to be comprised of a space-filling tiling of identical dodecahedral grains. Model grains creep following Norton's power-law. Additionally, grain boundary sliding, and accommodation of the interaction between slid neighbouring grains is considered. Cavitation and wedge-cracking on each of the twelve facets of the dodecahedral grain is permitted. Cavitational damage on different facets are allowed to interact, and promote, or inhibit each other. This model is able to accurately capture the dependence of the time to rupture on applied load in a 316 stainless steel. It is also able to predict whether failure will be brittle or ductile, and the elongation at failure, in good agreement with experiments [6].

The micro-mechanisms based model is computationally heavy and not naturally amenable to parallelisation. It is computationally infeasible, therefore, to embed it within, say a component level finite element simulation, in order to update the local damage state at each integration point. Simple continuum damage mechanical (CDM) models, e.g., Saanouni et al. [11], and Nikbin et al. [12], have long been used in this role. The CDM models are orders of magnitudes lighter than the detailed micro-mechanisms based model, in terms of the computational effort entailed. They represent material deterioration by a small number of variables (often just one) without taking individual micro-mechanisms into account. The value of this variable evolves irreversibly from zero to unity, where zero corresponds to the virgin state, and unity to the fully damaged state. In these models, damage is a conceptual variable, and cannot be correlated with experimentally measurable quantities.

A number of CDM models have been proposed in the literature, mostly on phenomenological considerations. Some of the more commonly used models are due to Kachanaov [13], Rabotnov [14], Liu and Murakami [15], Wen et al. [1], and Hayhurst et al. [16, 17]. On account of the simplicity of these models, and their different forms, they cannot all be expected to be good creep models of a particular material. It is the aim of this work to assess the goodness of the various CDM models by comparing their predictions with that of the detailed model, for austenitic stainless steel.

In the present work, it is assumed that the experimentally validated and detailed micro-mechanisms based model gives the correct reference deformation and damage behaviour. Five popular CDMs are summarised in Sec. 2. The deformation and damage parameters of each of the aforementioned CDM models is fit to the predictions of the detailed model at a high nominal stress level. CDM and micro-mechanisms based model predictions at intermediate nominal stress levels are then compared in Sec. 3. However, in the diffusion dominated low nominal stress regime, the Wen at al. [1] model also breaks down, and predicts highly non-conservative times to creep rupture. The cause for this breakdown is analysed presently, and a correction for the low nominal stress regime is proposed in Sec. 4.

2 Continuum Damage Models

2.1 The Kachanov-Rabotnov Model

Uniaxial forms of the constitutive equations of creep deformation and damage, given by Kachanov [13], and Rabotnov [14] are:

$$\frac{d\varepsilon}{dt} = B\left(\frac{\sigma}{1-D}\right)^n, \tag{1}$$

and

$$\frac{dD}{dt} = \frac{A}{q+1}\left(\frac{\sigma^p}{(1-D)^q}\right). \tag{2}$$

Here, ε denotes the uniaxial strain, t denotes time, σ denotes the tensile stress, and D denotes the damage parameter which increases monotonically from 0 to 1 as the damage progresses. B, n, A, p, and q represent material constants.

Eqs. (1) and (2) have been extensively used for analysing creep damage in structural components. But the form of the stress-enhancement due to damage, which scale as, $(1-D)^{-n}$ and $(1-D)^{-q}$, is inaccurate [15]. In creep tests, instantaneous elastic-plastic damage, and not creep damage, is the primary mode of fracture in the final stage of creep rupture [15]. Hence, Eqs. (1) and (2) end up in a position of representing elastic-plastic damage in terms of the creep-damage variable D, as $D \to 1$. These equations are therefore, not applicable in the tertiary creep regime.

2.2 The Liu and Murakami Model

In order to eliminate the aforementioned shortcomings in the Kachanov-Rabotnov model, Liu and Murakami [15] presented the following modification:

$$\frac{dD}{dt} = \frac{A}{q}\left[1 - \exp\left(-q\right)\right]\sigma^{p}\exp\left(qD\right). \tag{3}$$

Here, A, p and q are material constants. In order to describe the creep deformation, Liu and Murakami [15] also extended the micromechanics-based constitutive equation given by Hutchinson [18]. In uniaxial form, this is given by:

$$\frac{d\varepsilon}{dt} = B\sigma^{n}\exp\left[\frac{2\left(n+1\right)}{\pi\sqrt{1+\frac{3}{n}}}D^{\frac{3}{2}}\right], \tag{4}$$

where B and n are material constants.

2.3 The Wen, Tu, Gao and Reddy Model

Experimental studies [7, 19] on intergranular cavitation suggest that cavitational damage occurs on a surface normal to the direction of maximum principal tensile stress. This type of material degradation is modelled by a population of aligned penny-shaped cracks. Rodin et al. [20] developed a generalised structure of constitutive equations to describe deterioration of grain boundaries, by treating them as a non-dilute array of voids. Wen et al. [1] modified the Rodin and Parks equation to obtain a novel damage coupled creep constitutive equation. This modification brings the damage model predictions close to that of the finite element model investigated by Sester et al. [21] for two representative unit cells viz. cylindrical and body-centred cubic (BCC) cells, containing penny shaped micro-crack in the centre. In uniaxial form creep deformation and damage are given by:

$$\frac{d\varepsilon}{dt} = B\sigma_{eq}^{n-1}\left[\left(1+\beta\right)^{2}\right]^{\frac{n+1}{2}}, \tag{5}$$

and

$$\frac{dD}{dt} = A\frac{d\varepsilon}{dt}, \tag{6}$$

where

$$\beta(n,\rho) = \frac{2\rho}{n+1} + \frac{(2n+3)\rho^2}{n(n+1)^2} + \frac{(n+3)\rho^3}{9n(n+1)^3} + \frac{(n+3)\rho^4}{108n(n+1)^4},$$

,

$$\rho = \frac{n+1}{2\sqrt{1+\frac{3}{n}}}D^{3/2},$$

and A is a material parameter.

2.4 The Hayhurst, Vakili-Tahomi and Zhou Model

This model additionally accounts for the power law hardening for the primary creep regime, thereby describing the complete creep curve for low and high stresses [22]:

$$\begin{aligned} \frac{d\varepsilon}{dt} &= \frac{B}{(1-D)^n}\sinh\left(B^*\sigma(1-H)\right) \\ \frac{dH}{dt} &= \frac{h}{\sigma}\left(1-\frac{H}{H^*}\right)\frac{d\varepsilon}{dt} \\ \frac{dD}{dt} &= A\frac{d\varepsilon}{dt} \end{aligned} \tag{7}$$

Here, H, the strain hardness increases from zero to the value H^* at beginning of secondary creep. H^*, and h determine the response during primary creep. B and B^* correspond to secondary creep. A refers to the tertiary creep. The damage variable D evolves during tertiary creep. It increases from 0 to $1/3$.

2.5 The Hayhurst, Dyson and Lin Model

This model employs the skeletal stress technique for the prediction of creep lifetime. The skeletal stress technique addresses the stress redistribution that results after completion of primary creep and during secondary creep in the absence of tertiary creep [17]. Othman et al. [23] improved the model to account for the stress redistribution due to tertiary creep which results in material weakening. Later, for application to nickel superalloy and many other alloy systems, an extra damage parameter was introduced along with the proposition of equations containing stress dependence of creep rate as following a hyperbolic sine function [24]. The damage parameter D_1 represents dislocation softening and evolves from 0 to 1. D_2 represents nucleation controlled creep constrained and evolves from 0 to $1/3$, as in Sec. 2.4.

The deformation and damage evolution equations are:

$$
\begin{aligned}
\frac{d\varepsilon}{dt} &= \frac{B}{(1-D_1)(1-D)^n}\sinh(B^*\sigma) \\
\frac{dD_1}{dt} &= \frac{CD_1}{(1-D)^n}\sinh(B^*\sigma) \\
\frac{dD}{dt} &= A\frac{d\varepsilon}{dt}.
\end{aligned}
\tag{8}
$$

2.6 The micro-mechanisms based model

In the micro-mechanisms based model [25], the initial microstructure is idealised as a space-filling tiling of identical rhombic dodecahedral grains, shown in the Fig. 1. When subjected to constant uniaxial nominal stress, σ, each grain creeps following Norton's law [26]. Additionally, grains can slide past each other. Damage takes the form of cavities and wedge cracks developed along the grain boundaries. The extent of the damage is parameterised by the cavity and wedge crack lengths. They evolve with time, following a law that aims to minimise the free energy of the grain. The free energy expression accounts for grain boundary sliding, and for the mechanical interaction between the facets of the dodecahedral grain. Creep rupture corresponds to the complete damage of two adjacent facets of the grain.

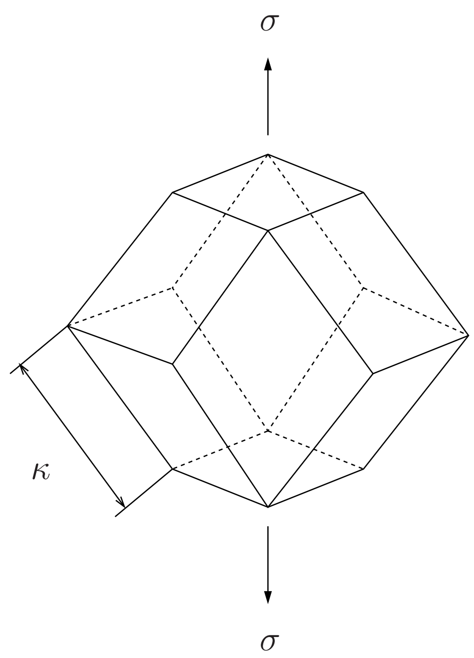

Fig. 1: A rhombic dodecahaedral grain in the micro-mechanisms based model [25] under uniaxial tension. The polycrystal is obtained by tiling this grain throughout space. κ is a characteristic grain dimension.

3 Results

Material constants for AISI 316 steel, associated with each of the models described in Sec. 2 have been selected so that the minimum creep rate and time to rupture match those predicted by the micro-mechanisms based model at nominal stress $\sigma = 295$ MPa. The temperature is fixed at 873 K. The resulting values of the material constants are given in Table 1.

The models under study have been abbreviated as K-R, L-M, W-T-G-R, H-V-Z and H-D-L for the Kachanov-Rabotnov, Liu-Murakami, Wen-Tu-Gao-Reddy, Hayhurst-Vakili Tahami-Zhou and Hayhurst-Dyson-Lin models, respectively. All the models reasonably cap-

Table 1: Material constants for various CDM models fit to capture the creep rate, and time to rupture, predicted by the micro-mechanisms based model at nominal stress $\sigma = 295$ MPa.

	parameter [units]	K-R	L-M	W-T-G-R	H-V-Z	H-D-L
Creep exponent	n	11	11	7.61	-	-
Secondary Creep	B [MPa^{-n}s^{-1}]	3.8×10^{-34}	6×10^{-34}	9×10^{-26}	8×10^{-11}	8.5×10^{-11}
Primary creep	$H*$	-	-	-	4.26×10^{-1}	-
	h	-	-	-	4×10^{4}	-
Damage	A [MPa^{-p}s^{-1}]	3.1×10^{-13}	1.5×10^{-13}	4.545	9.1	3.8
	C	-	-	-	-	1.06×10^{-8}
Other	p	2.6	2.74	-	-	-
	q	5	6	-	-	-
	B^{*} [MPa^{-1}]	-	-	-	4.24×10^{-2}	2.5×10^{-2}

ture both the minimum creep rate, and the creep lifetime predicted by the micro-mechanisms based model, as shown in Fig. 2.

Keeping the material parameters fixed, Fig. 3 compares the predictions of the micro-mechanisms based model and the CDM models at the higher applied stress level of 350 MPa. It is seen that the K-R, L-M, and W-T-G-R models still agree well with the micro-mechanisms based model's predictions. This not surprising considering that both 295 MPa, and 350 MPa fall within the regime of ductile fracture at the temperature of interest. In this regime, the creep lifetime is determined by the secondary creep rate [5], which are similarly represented in the micro-mechanisms based model, and in the K-R, L-M, and W-T-G-R CDM models. The H-V-Z and H-D-L models, however, represent the creep rate, $d\varepsilon/dt$ using a hyperbolic sine functional form. This makes the creep rate predicted by the latter models less sensitive to the applied stress level, and causes the H-V-Z and H-D-L models to under-predict the creep rates. Nevertheless they too predict the creep lifetimes fairly accurately.

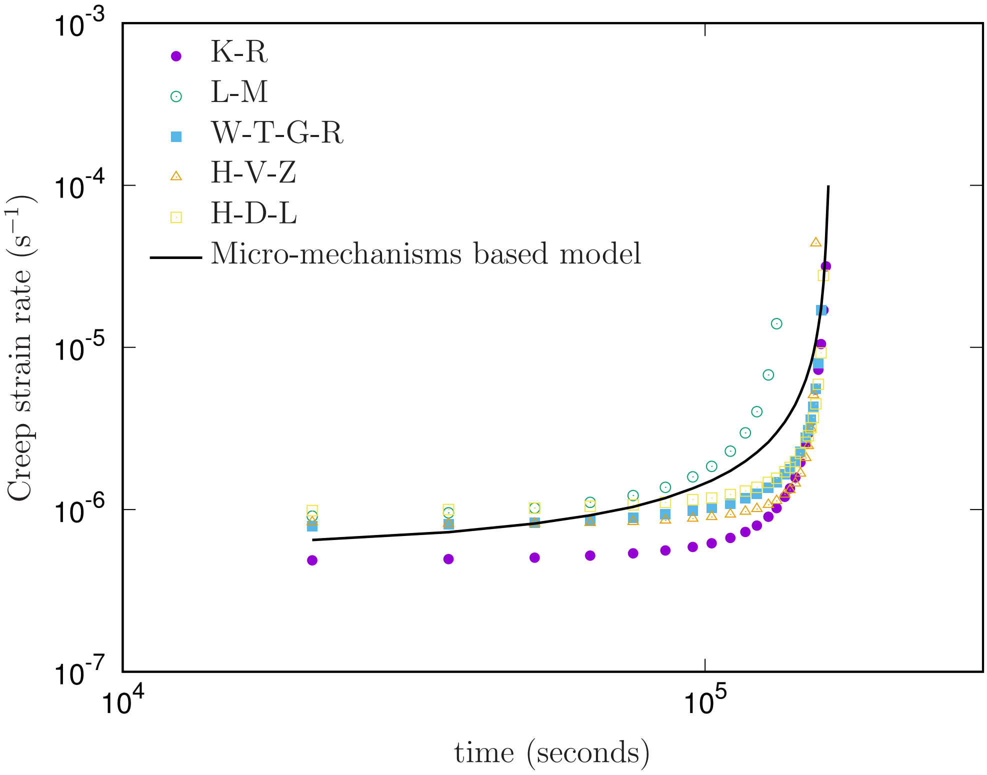

Fig. 2: Time history of the strain-rate predicted by the five CDM models at a nominal uniaxial stress of $\sigma = 295$ MPa. Material parameters are fit to values given in Table 1 so that all models predict approximately the same creep rate histories, and time to failure.

Attention is next turned to the nominal uniaxial stress level of 125 MPa, which is lower than that used for fitting the parameters of the CDM models. The predictions of the five CDM models and that of the micro-mechanisms based model are shown in Fig. 4. Among the five models considered, the prediction of the Wen et al. [1] model agrees best with that of the micro-mechanisms based model. The H-D-L and the H-V-Z models overestimate the minimum creep strain rate, and underestimate the time to failure. Again, this is because the hyperbolic sine functional form of the creep rate in the H-D-L and H-V-Z models makes the creep rate less sensitive to the applied stress. The K-R and L-M models underestimate both

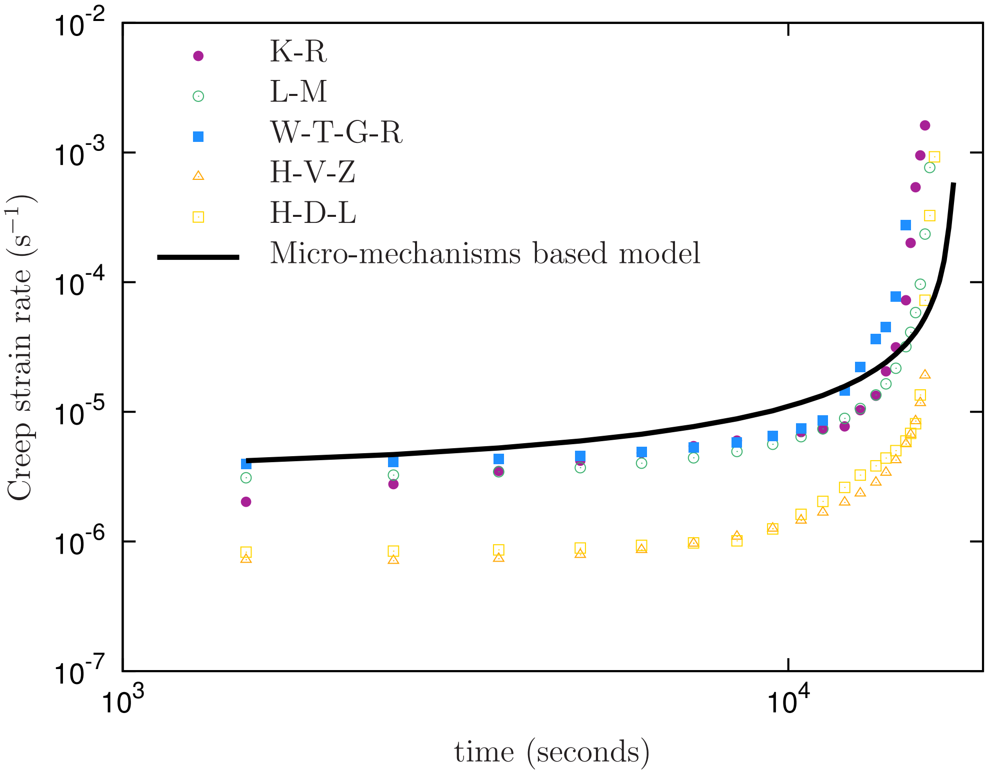

Fig. 3: Time history of the strain-rate predicted by the five CDM models at a nominal uniaxial stress of $\sigma = 350$ MPa. Material parameters are fixed at the values given in Table 1.

the creep rate, and the time to failure by far. Although not shown, these observations hold for all nominal stress levels between 295 MPa and 125 MPa.

At the still lower nominal uniaxial stress level of 55 MPa, the strain history predicted by the Wen et al. [1] and by the micro-mechanisms based model are compared in Fig. 5. While the strain-rates predicted by both models are small, the time to failure predicted by the Wen et al. model is non-conservative by over two orders of magnitude.

The times to failure predicted by the Wen et al. [1] model are compared with that predicted by the micro-mechanisms based model at various nominal uniaxial stress levels in Fig. 6. The model predictions agree well for $\sigma \geq 125$ MPa. At lower stress levels, though,

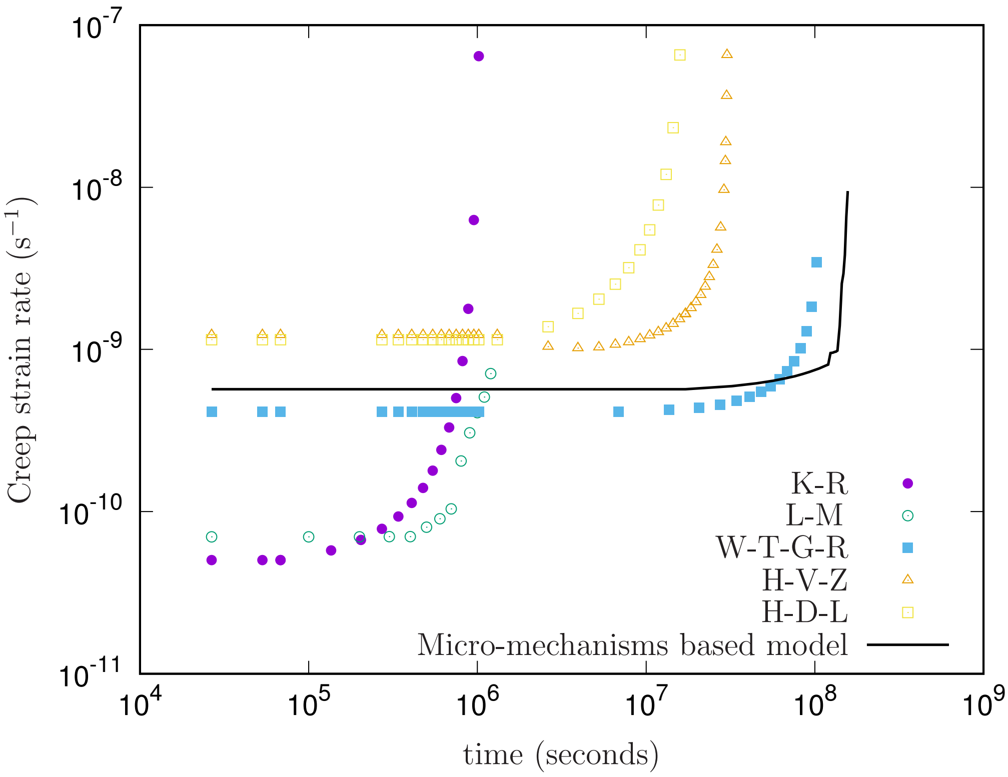

Fig. 4: Time history of the strain-rate predicted by the five CDM models. Model parameters are held fixed at the values given in Table 1. The nominal uniaxial stress is $\sigma = 125$ MPa. The predictions of the Wen et al. [1] model agree well with that of the micro-mechanisms based model.

the time to failure predicted by the Wen et al. model is progressively greater than that predicted by the micro-mechanisms based model.

4 Discussion

Of the five continuum damage models considered, the Wen et al. [1] model predicts the creep-rate and time to failure of AISI 316 specimens at 873 K in best agreement with a

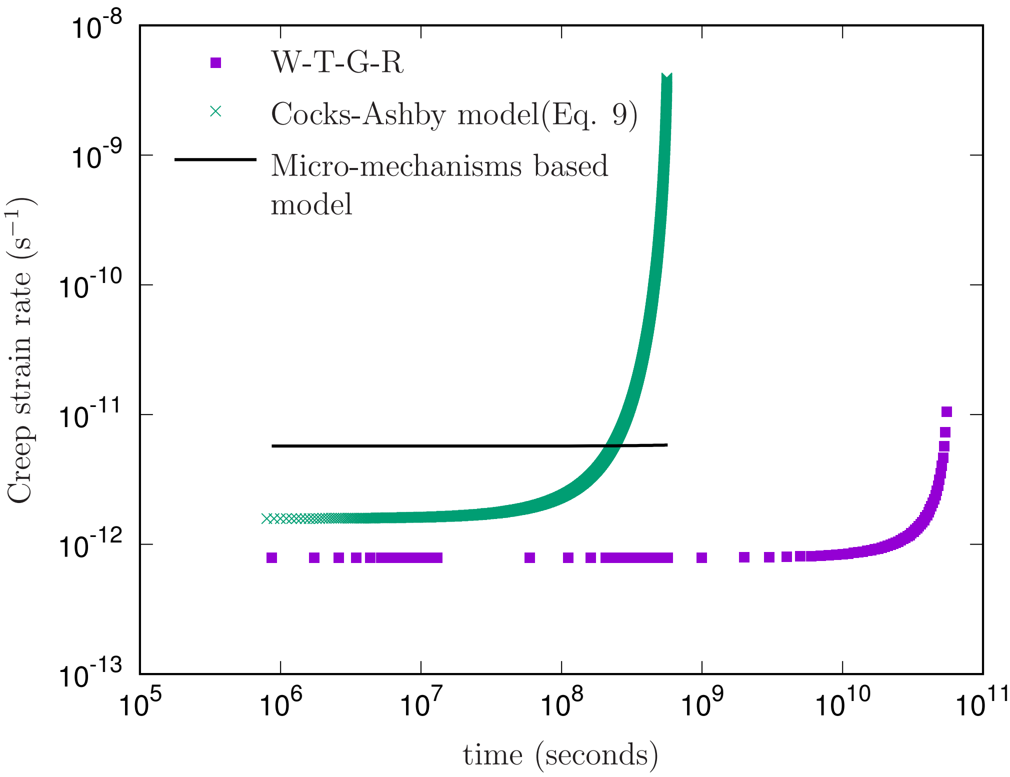

Fig. 5: Time history of the strain-rate predicted by the Wen et al. [1] and micro-mechanisms based models. Model parameters are held fixed at the values given in Table. 1. The nominal uniaxial stress is $\sigma = 55$ MPa. The Wen et al. model overestimates the time to failure by far.

validated micro-mechanisms based model. This agreement is good for nominal uniaxial stress levels ≥ 125 MPa. At lower stress levels, though, the Wen et al. model overestimates the time to failure significantly. This is because, failure in the Wen et al. model occurs by creep-ductility exhaustion. In the micro-mechanisms based model, however, failure occurs due to constrained diffusional cavity growth.

For constrained cavity growth at low stress levels, Cocks and Ashby [2] have proposed:

$$\frac{dD}{dt} = \frac{K}{\sqrt{D}\log(1/D)}\sigma. \tag{9}$$

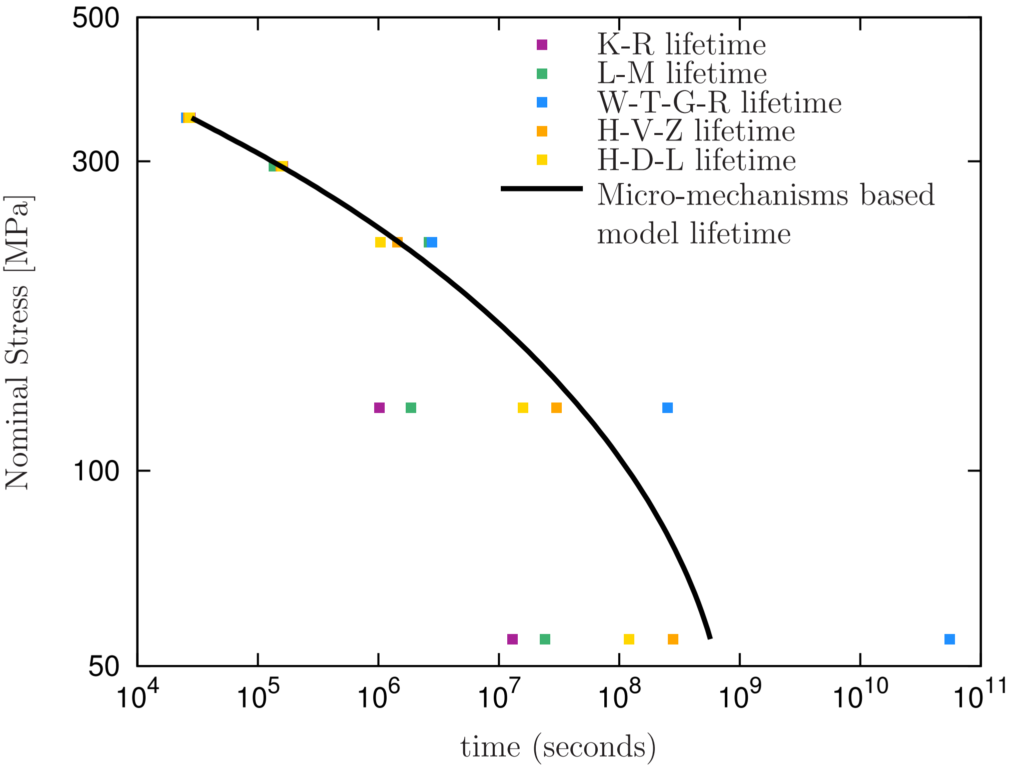

Fig. 6: Time to rupture predicted by the five models of present study at various stress levels σ. Note that the W-T-G-R model agrees best for $\sigma \geq 125$ MPa, but overestimates the time to failure at $\sigma = 55$ MPa by two orders of magnitude.

Here, the damage variable D is identified with the area fraction of voids, and defined as $D = r_h^2/l^2$. r_h and l are the radius of growing voids and half of the centre-to-centre distance between two voids, respectively. Setting $K = 1.4223 \times 10^{-5}$ / MPa-s, matches the time to failure predicted by the micro-mechanisms based model in the uniaxial stress-range of 55 to 95 MPa. This is shown in Fig. 7. It is also seen that the lower envelope of the times to rupture predicted by the Wen et al. [1] model and the Cocks-Ashby models captures the full range of the times to ruptures obtained from the micro-mechanisms based model.

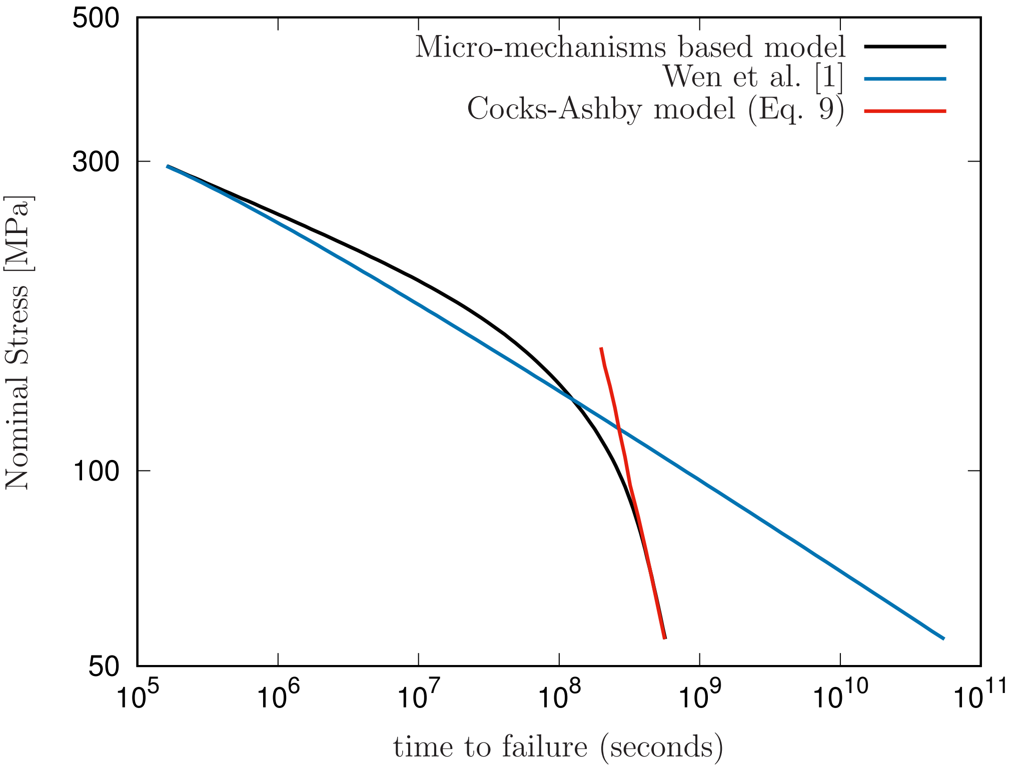

Fig. 7: Time to rupture predicted by the Wen et al. [1] model, based on creep ductility exhaustion and by the Cocks and Ashby [27] model, based on diffusional cavity growth. The micro-mechanisms based model's time to rupture is well captured by the more conservative of these two models.

The present study has focussed on the regime of nominal stresses less than 295 MPa. It is natural to ask about how the predictions of the micro-mechanisms based and continuum damage models may compare at nominal stresses in excess of 295 MPa.

5 Conclusions

Finite element based creep simulations on macroscopic components require a computationally light creep deformation and damage model to implement at integration points. It is infeasible to use a computationally intensive model such as the validated micro-mechanisms based model [25] for this purpose. Instead, it is preferred to use a continuum damage model (CDM).

The most appropriate CDM model must be able to capture the principal damage mechanisms over the temperature and stress range, for the material of interest. Five CDM models have been evaluated against the predictions of a detailed micro-mechanisms based model, for AISI 316 steel. The model due to Wen et al. [1] best captures the times to rupture obtained from the micro-mechanisms based model in the stress regime wherein creep ductility exhaustion is a valid assumption. At lower stresses, the Cocks and Ashby [2] model serves as a good approximation. It is recommended to take the lower envelope of these two models in component level simulations as a good computationally light approximation of the material creep response.

Acknowledgements The authors thank the High Performance Computing Centre at IIT Madras, where the simulations reported here were performed. We also gratefully acknowledge helpful comments from the referee.

References

1. Jian-Feng Wen, Shan-Tung Tu, Xin-Lin Gao, and JN Reddy. Simulations of creep crack growth in 316 stainless steel using a novel creep-damage model. *Engineering Fracture Mechanics*, 98:169–184, 2013.
2. ACF Cocks and MF Ashby. On creep fracture by void growth. *Progress in Materials Science*, 27(3-4):189–244, 1982.
3. D. A. Miller and T. G. Langdon. Creep fracture maps for 316 stainless steel. *Metall. mater. trans.*, 10A:1635–1641, 1979.

4. H. J. Frost and M. F. Ashby. *Deformation mechanism maps*. Pergamon press, Oxford, 1982.
5. N. J. Hoff. The necking and the rupture of rods subjected to constant tensile loads. *J. Appl. Mech.*, pages 105–108, 1953.
6. G. Sasikala, S. L. Mannan, M. D. Mathew, and K. Bhanu Rao. Creep deformation and fracture behavior of types 316 and 316L(N) stainless steels and their weld metals. *Metal. mater. trans*, 31(4):1175–1185, 2000.
7. I.-W. Chen and A. S. Argon. Creep cavitation in 304 stainless steel. *Acta metall.*, 29(7):1321–1333, 1981.
8. I.-W. Chen. Cavity growth on a sliding grain boundary. *Metall. mater. trans.*, 14A:2289–2293, 1983.
9. B. F. Dyson. Constraints on diffusional cavity growth rates during creep. *Metal. Sci.*, 10(349–353), 1976.
10. S Mahesh, KC Alur, and MD Mathew. A creep model for austenitic stainless steels incorporating cavitation and wedge cracking. *Modelling and Simulation in Materials Science and Engineering*, 19(1):015005, 2010.
11. K Saanouni, J. L. Chaboche, and C. Bathias. On the creep crack growth prediction by a local approach. *Eng. Fract. Mech.*, 25(5):677–691, 1986.
12. KM Nikbin, DJ Smith, and GA Webster. Prediction of creep crack growth from uniaxial creep data. *Proc. R. Soc. Lond. A.*, 396(1810):183–197, 1984.
13. LM Kachanov. Time of the rupture process under creep conditions. *Isv. Akad. Nauk. SSR. Otd Tekh. Nauk*, 8:26–31, 1958.
14. Y. N. Rabotnov. *Creep problems in structural members*, volume 7. North-Holland Pub. Co., 1969.

15. Yan Liu and Sumio Murakami. Damage localization of conventional creep damage models and proposition of a new model for creep damage analysis. *JSME International Journal Series A*, 41(1):57–65, 1998.

16. DR Hayhurst, F Vakili-Tahami, and JQ Zhou. Constitutive equations for time independent plasticity and creep of 316 stainless steel at 550 c. *International journal of pressure vessels and piping*, 80(2):97–109, 2003.

17. DR Hayhurst, BF Dyson, and J Lin. Breakdown of the skeletal stress technique for lifetime prediction of notched tension bars due to creep crack growth. *Engineering fracture mechanics*, 49(5):711–726, 1994.

18. JW Hutchinson. Constitutive behavior and crack tip fields for materials undergoing creep-constrained grain boundary cavitation. *Acta Metallurgica*, 31(7):1079–1088, 1983.

19. DR Hayhurst. On the role of creep continuum damage in structural mechanics. *Pineridge Press, Engineering Approaches to High Temperature Design*, pages 85–176, 1983.

20. Gregory J Rodin and David M Parks. A self-consistent analysis of a creeping matrix with aligned cracks. *Journal of the Mechanics and Physics of Solids*, 36(2):237–249, 1988.

21. Matthias Sester, Ralf Mohrmann, and Hermann Riedel. A micromechanical model for creep damage and its application to crack growth in a 12% cr steel. In *Elevated Temperature Effects on Fatigue and Fracture*. ASTM International, 1997.

22. Qiang Xu and DR Hayhurst. The evaluation of high-stress creep ductility for 316 stainless steel at 550 c by extrapolation of constitutive equations derived for lower stress levels. *International journal of pressure vessels and piping*, 80(10):689–694, 2003.

23. AM Othman and DR Hayhurst. Determination of large strain multi-axial creep rupture criteria using notched-bar data. *International Journal of Damage Mechanics*, 2(1):16–

52, 1993.

24. AM Othman, DR Hayhurst, and BF Dyson. Skeletal point stresses in circumferentially notched tension bars undergoing tertiary creep modelled with physically based constitutive equations. *Proceedings of the Royal Society of London A: Mathematical, Physical and Engineering Sciences*, 441(1912):343–358, 1993.
25. S. Mahesh, K. C. Alur, and M. D. Mathew. A creep model for austenitic stainless steels incorporating cavitation and wedge cracking. *Modeling simul. mater. sci eng.*, 19(1):015005, 2011.
26. F. H. Norton. *Creep of steel at high temperatures*. McGraw Hill, 1929.
27. A. C. F. Cocks and M. F. Ashby. On creep fracture by void growth. *Prog. mater. sci.*, 27(3–4):189–244, 1982.